JOURNAL OF AIRCRAFT
Vol. 35, No. 6, November–December 1998

Behavior of Compression-Loaded Composite Panels with Stringer Terminations and Impact Damage

Dawn C. Jegley*
NASA Langley Research Center, Hampton, Virginia 23681-2199

The results of an analytical and experimental study of graphite–epoxy stiffened panels with impact-damaged stringer terminations are presented. Five stitched graphite–epoxy panels with stiffeners with a gradual reduction in either thickness or height were examined. Panels were analyzed using finite element analysis and tested by loading them in axial compression to a predetermined load. The panels were then subjected to impact damage and loaded to failure. Axial midplane strains, surface strains, interlaminar strains, and failure results are discussed.

Introduction

ONE of the goals of the NASA Advanced Composites Technology Program (ACT) was to develop the technology needed for future low-cost, lightweight composite structures for commercial transport aircraft. One material system that has the potential of reducing the weight and cost of commercial transport aircraft structure is a stitched graphite–epoxy material system. By using stitches through the thickness of a low-cost graphite–epoxy material system, the labor associated with wing cover panel fabrication and assembly can be significantly reduced. When the entire wing cover panel is stitched together, including stringers, intercostals, and spar caps, the need for mechanical fasteners is almost eliminated, which significantly reduces part count and, therefore, cost. However, to take advantage of this material system, problems associated with impact damage must be understood and resolved. Damage tolerance characteristics of composite materials can be improved by using advanced resin systems, but the currently available resins that provide improved damage tolerance are prohibitively expensive for use in low-cost commercial aircraft. Composite panels fabricated with low-cost resins usually have degraded strength capability when subjected to low-speed impact damage, such as hail damage. By using stitches through the thickness of a low-cost graphite–epoxy material system, damage propagation is reduced, and improved damage tolerance is possible. One critical consideration for evaluating the effect of impact damage on a graphite–epoxy wing is the effect of impact damage in stiffener termination regions that have significant local stress gradients.

To evaluate the effect of impact damage on the response of composite panels with stiffener terminations, five panels were cut from undamaged regions of a 12-ft-long, stitched graphite–epoxy wing box. This wing box was fabricated by the McDonnell Douglas Aerospace Company as part of the NASA Advanced Composites Technology Program and was loaded to failure at the NASA Langley Research Center. A complete description of the wing box is presented in Ref. 1. Panels used in the present study have stringers with a gradual reduction or taper in either thickness or height. The panels were analyzed using finite element analysis methods, and they were tested by loading the panels in axial compression to a predetermined load. The panels were then subjected to impact damage and loaded to failure to determine their residual strength.

Received April 6, 1998; revision received June 15, 1998; accepted for publication June 30, 1998.

*Senior Aerospace Engineer, Structural Mechanics Branch, Structures Division, M/S 190. Senior Member AIAA.

Panel Descriptions

Two single-stringer panels and three multistringer panels were cut from the McDonnell Douglas wing box. All panels were fabricated from Hercules, Inc., AS4/3501-6 and IM7/3501-6 graphite–epoxy materials that were stitched together using E. I. DuPont de Nemours, Inc., Kevlar® thread. IM7 graphite fibers were only used for the 0-deg fibers in the skin of the multistringer panels. The composite skin and stiffeners were composed of layers of the graphite material forms that were prekitted in nine-ply stacks. Each nine-ply stack had a $[45/-45/0_2/90/0_2/-45/45]_T$ laminate stacking sequence and was approximately 0.058 in. thick. Several nine-ply stacks of the prekitted material were used to build up the desired thickness at each location. The composite wing box was fabricated using the resin film infusion (RFI) process.[2]

Single-stringer panels with centrally located stringers were cut from the upper cover panel of the wing box and are designated as panels U-1 and U-2 herein. Panel U-1 is shown in Fig. 1. Multistringer panels were cut from the lower cover panel of the wing box and are designated as L-1, L-2, and L-3 herein. Panel L-2 is shown in Fig. 2.

The stringers and intercostals are blade stiffeners that are ~2.3 in. tall in the single-stringer panels, and 2.0 in. tall in the multistringer panels. All stringer blades in the panels are nominally 0.46 in. thick (eight stacks) with a 1.12-in.-wide flange on either side of the web. All intercostal blades are nominally 0.116 in. thick (two stacks) with a 1.1-in.-wide flange on either side of the web. The flange thickness is half the blade thickness. Intercostals are perpendicular to the stringers. A graphite–epoxy rib was bolted to each intercostal in the original wing box. This rib was cut to match the height of the intercostal for these single- and multistringer panels rather than risk damaging the intercostals by removing the bolts. Because of concerns that the stiffener-termination or runout region would fail prematurely in the wing box test, a row of bolts was added to each flange of a terminating stringer to prevent the stringer flange from separating from the skin.

The geometry of the single-stringer panels is shown in Fig. 3. For the single-stringer panels, the stringer blade is eight stacks thick at the thicker end and two stacks thick at the termination point or thinner end. Stacks are terminated on both

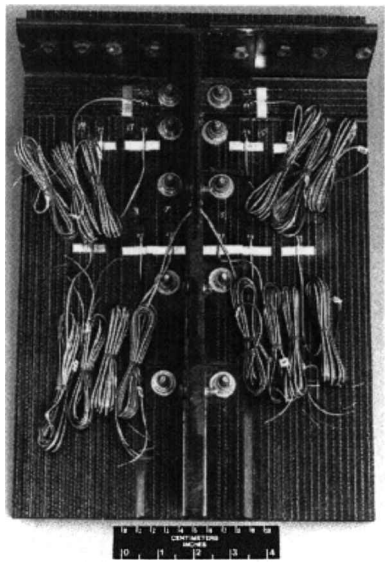

Fig. 1 Photograph of single-stringer panel U-1 prior to testing.

Fig. 2 Photograph of multistringer panel L-2 prior to testing.

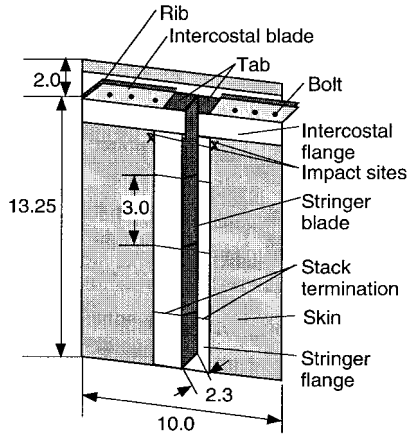

Fig. 3 Geometry of a single-stringer panel. Length dimensions are in inches.

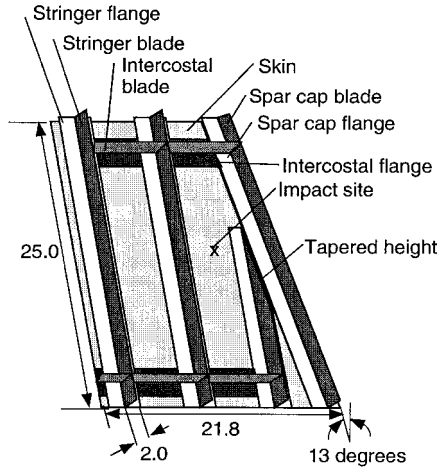

Fig. 4 Geometry of a multistringer panel. Length dimensions are in inches.

sides of the blade at 3-in. intervals. Stringer flanges are always half the thickness of the blade. The stringer blade terminates at the intercostal by folding out into tabs that are placed against the intercostal blade as shown in Fig. 3. Additional bolts were added to the stringer blade to prevent the blade from delaminating prematurely in the wing box test. The single-stringer panels are 15.25 in. long and 10.0 in. wide with the intercostal located 2 in. from one end of the panel. The only difference between the two single-stringer panels is that the entire skin of panel U-1 is five stacks thick while the skin of panel U-2 is five stacks thick over approximately half the width of the panel and six stacks thick for the rest of the panel.

The geometry of the multistringer panels is shown in Fig. 4. The multistringer panel skins range in thickness from six to eight stacks. Each multistringer panel has two eight-stack-thick stringers along the full length of the panel and one eight-stack-thick stringer that tapers from the full stringer height of 2.0 in. over a distance of 7.5 in. Stringer flanges remain four stacks thick for the entire stringer length. The spar cap, which is the same height as the stringers, runs the length of the panel and is oriented at an angle of 13 deg to the stringers. In the original wing box, graphite–epoxy ribs and spars were bolted to the intercostals and spar caps, respectively. For the multistringer panels, the rib and spar were cut to the same height as the intercostals. The tapered stringer terminated at the flange of the spar cap, as shown in Fig. 4. The multistringer panels are between 21 and 25 in. long and 21.8 in. wide at one end. The other end is between 16.25 and 17.25 in. wide.

The loaded edges of all specimens were potted in an epoxy compound that was 1 in. deep to simulate clamped end conditions. These ends were ground flat and parallel to each other prior to testing.

Impact Damage

Damage was inflicted on the unstiffened side of the panels with a 1-in.-diam. tup. The level of damage was defined by the amount of permanent indentation or dent depth. A dent that is more than 0.1 in. deep is assumed to be visible. Damage size was also measured using an ultrasonic C-scan procedure. The dent depth and damage size are listed in Table 1 for each panel. Panel U-1 was not damaged and panel U-2 was damaged at two locations. The other three panels were each impacted at one location.

All multistringer panels have a thick layer of resin on the unstiffened surface. Indentation depth for these panels is based on a measured indention at the impact site, less the thickness of the surface resin layer. The thickness of the surface resin was determined by measuring the thickness removed where fasteners were added at the adjacent tapered stiffener during assembly of the wing box. Extra surface resin thicknesses on the multistringer panels ranged from 0.02 to 0.07 in.

Table 1 Damage description

Panel	Damage depth, in.	Damage size, in.
Single-stringer		
U-1	——	——
U-2	0.155	3.8 × 2.2
	0.155	2.0 × 0.9
Multistringer		
L-1	0.163	5.2 × 3.0
L-2	0.108	4.0 × 2.1
L-3	~0	~0

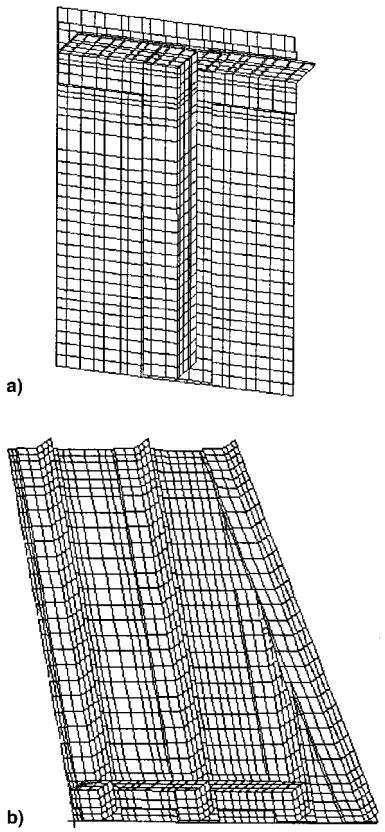

Fig. 5 Finite element models: a) single- and b) multistringer model.

Loading and Instrumentation

All panels were loaded in axial compression. Knife-edge supports were used on the unloaded edges of panels U-1 and U-2 to minimize out-of-plane motion of the skin. No support was provided for the intercostal or intercostal flange. No edge supports were used for testing the multistringer panels. Panels to be damaged were first loaded to a predetermined load level and then the load was removed to acquire deflection and strain information of an undamaged structure for comparison with analysis and to assist in evaluating the effect of damage. The panels then were impact damaged and loaded to failure. Panels were instrumented with strain gauges near and away from the impact sites. Direct current displacement transducers (DCDTs) were used to monitor end-shortening and out-of-plane displacements.

Load rates were ~10,000 lb/min for the single-stringer panels and ~80,000 lb/min for the multistringer panels.

Analysis

A geometrically nonlinear analysis of each panel was conducted with the finite element code STAGS.[3] A unique model was created for each panel so that all differences in skin thickness and geometry could be considered. The models used for panels U-1 and L-1 are shown in Fig. 5. Similar models were used for the other panels tested.

Material properties used in the analysis are shown in Table 2. Intercostals and ribs were included in the models where appropriate; however, fasteners through the skin were not included in any of the finite element models. Stringer and intercostal flanges were modeled separately from the skin for all finite element models, and eccentricities were used to offset elements with thicker skin to account for changes in skin thickness so that the models would accurately reflect these details.

Results

Experimental and analytical results for the study of two single-stringer panels and three multistringer panels are presented in this section, and panel failure results are summarized in Table 3. In graphical comparisons between experimental and analytical results, experimental results are shown as solid lines and analytical results are shown as dashed lines.

Single-Stringer Panels

Two single-stringer panels, identified herein as U-1 and U-2, were loaded to failure. Panel U-1 was not impact damaged.

The axial surface strains in the skin of panel U-1 at a distance 4.75 in. away from the intercostal are shown in Fig. 6. Results from back-to-back strain gauges agree well with each other, indicating that little bending occurs away from the intercostal. The axial strains in the skin at the edge of the intercostal flange are shown in Fig. 7. Experimental and analytical results indicate that bending behavior occurs in the region of the intercostal flange. Analytical and experimental results are in good agreement.

Analytically determined axial surface strains for a load of 100,000 lb are shown in Fig. 8 for panel U-1. The maximum compressive axial surface strain occurs in the region of highest bending, which is in the intercostal flange near the intercostal. In this region the blade is only two stacks thick and it passes over the intercostal flange without connecting to it. As can be seen in Fig. 3, the stringer flange terminates at the edge of the intercostal flange, allowing more bending to occur. The maximum axial strain at the laminate midplane is less effected by bending behavior and occurs in the stringer flange near the intercostal. Based on an allowable axial strain value at the laminate midplane for an undamaged structure of 0.0093 in./in., failure should not occur because of axial strain for a load less than 108,500 lb. Lateral strains were small enough to have little effect on failure. However, the shear strain in the intercostal flange is predicted to exceed the shear strain allowable of 0.0126 in./in. for loads greater than 91,200 lb. Shear strain in the intercostal flange causes or contributes to failure of the panel because the panel failed at 98,200 lb.

The predicted interlaminar stresses, normalized by material failure stresses, can be combined to evaluate interlaminar stresses between flanges and skin.[4] The assumed interlaminar tensile normal stress at failure, F_z = 5.9 ksi, and the assumed interlaminar shear stress at failure, F_s = 13.5 ksi, are used to obtain an interlaminar failure parameter. A normalized interlaminar failure prediction is obtained by using the equation

$$I = [(\sigma_z/F_z)^2 + (\tau_{xz}/F_s)^2 + (\tau_{yz}/F_s)^2]^{1/2}$$

where σ_z is the normal stress and τ_{xz} and τ_{yz} are the interlaminar shear stresses. Based on this normalization, any value of the interlaminar failure parameter greater than 1.0 could signify that failure occurs at the corresponding location. This parameter is used in a qualitative sense to give failure location and to indicate the likelihood of a failure rather than to predict a failure load because further work should be done to improve

Table 2 Material properties

Property	Stitched AS4/3501-6 (panels U-1 and U-2)	Stitched AS4/IM7/3501-6 (panels L-1, L-2, and L-3)
Longitudinal stiffness	8.17×10^6 psi	9.98×10^6 psi
Transverse stiffness	4.46×10^6 psi	4.45×10^6 psi
Shear stiffness	2.35×10^6 psi	2.57×10^6 psi
Poisson's ratio	0.458	0.409

Table 3 Summary of panel failure results

Panel	Failure load, lb	Failure load prediction using PDF parameter, lb	Primary cause of failure	Design stress,[a] ksi	Failure stress at impact site, ksi	Maximum stress in skin at failure, ksi	Load at which design stress occurs at impact site, lb
U-1	99,200	No damage	Interlaminar and shear strain	37.5	No damage	32.2	——
U-2	94,600	95,547	Axial strain at impact site	37.5	29.4	29.4	120,500
L-1	435,000	640,000	Axial strain at impact site	39.4	35.2	51.0	487,087
L-2	484,000	570,000	Axial strain at impact site	39.4	44.6	59.6	428,307
L-3	610,000	640,000	Axial strain at impact site	43.5	50.0	66.0	529,319

[a]Based on skin thickness and McDonnell Douglas Aerospace criterion.

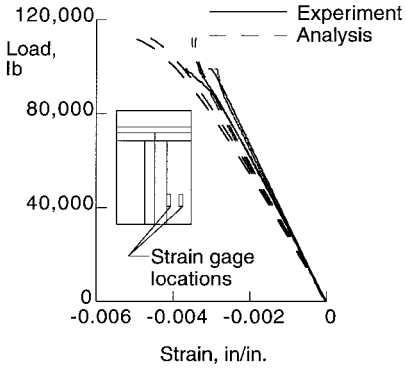

Fig. 6 Axial far-field strain in the skin of panel U-1.

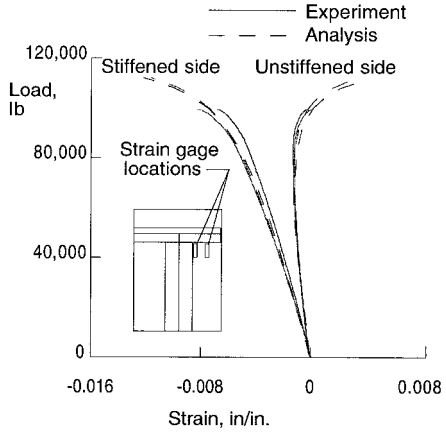

Fig. 7 Axial strain in skin near the intercostal flanges for panel U-1.

the accuracy of interlaminar shear and normal allowables in stitched structure.

The values of the interlaminar failure parameter is shown in Fig. 9 for the interface between the skin and the stringer flange of panel U-1. The maximum interlaminar stress in the stringer flange occurs at the end of the flange, where it teminates at the intercostal flange. At this location the interlaminar failure parameter is approximately equal to 2.0 for a load of 100,000 lb. The maximum axial strain, shear strain, and interlaminar shear strain occur in close proximity, and failure could result from a combination of strains.

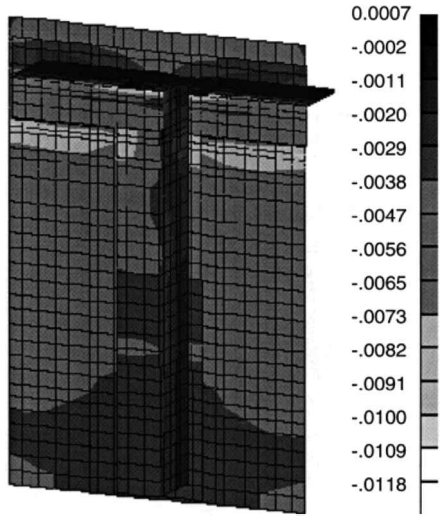

Fig. 8 Axial surface strain for a load of 100,000 lb for panel U-1.

Test results indicate that failure in panel U-1 initiates at the interface between the skin and stringer flange. The separation of the stringer flange from the skin occurs immediately beneath the blade of the stringer near the termination of the stringer flange. As load increases, separation between the stringer flange and skin progresses down the panel, away from the intercostal. The analytical prediction of the location of the initial failure agrees with the experimental results. The panel failed at 99,200 lb of load.

Panel U-2 was initially loaded to 83,000 lb. The panel was not damaged during the initial loading. The panel was unloaded and damaged in two locations, each with dent depths of approximately 0.15 in. The resulting damage was clearly visible. Descriptions of the damage are presented in Table 1.

Results for end-shortening and out-of-plane displacements for panel U-2 during the preliminary (undamaged) loading, and as predicted by finite element analysis, are shown in Fig. 10. Out-of-plane displacements were measured 5.5 in. from the bottom of the panel near the knife edge support and 10.6 in. from the bottom of the panel in three locations across the width of the panel. Analytical and experimental results are in good agreement.

After being subjected to impact damage, the panel was loaded to failure. The impact damage had little effect on the

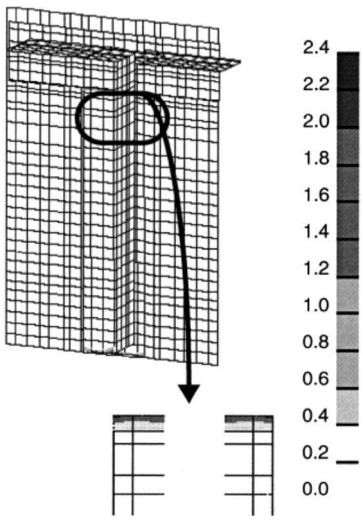

Fig. 9 Normalized interlaminar stresses at skin-to-stringer flange interface for a load of 100,000 lb for panel U-1.

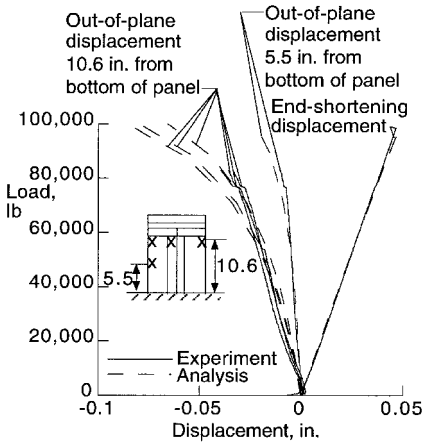

Fig. 10 Displacement results for undamaged panel U-2. All dimensions are in inches. *x* represents the location of out-of-plane displacement measurement.

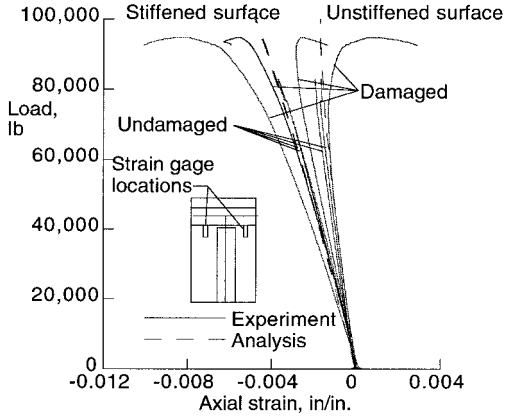

Fig. 11 Axial strains near the intercostal flange in panel U-2.

far-field behavior, or on the global behavior, of the panel. The local effect of the impact damage can be seen in Fig. 11, where results are shown for strain gauges within 1 in. of the impact sites. Surface damage closer than 1 in. from the impact site was too severe to allow strain measurements.

The allowable midplane strain assumed for damaged structure is 0.0053 in./in. The analysis of the undamaged structure predicts a strain at the impact site of 0.0053 in./in. for a load of 147,000 lb. Failure through the impact site would not be expected for loads less than 147,000 lb. Because the failure load is significantly less than 147,000 lb, the midplane strain at the impact site cannot be used to predict failure of this panel.

Ideally, a panel with a 0.1-in.-deep indentation (caused by impact damage) will not fail when subjected to a load that causes a stress less than the design stress at the reference surface of the skin at the indentation site. The design stress is affected by the skin thickness. Based on a design stress of 37.5 ksi for the five-stack-thick region of the panel, a failure load greater than 120,000 lb would be expected. The panel failed with a stress of 29.4 ksi at the impact site, which is approximately 21% less than the design stress. However, the panel was damaged with dents that were 50% deeper than the 0.1-in.-deep dent-depth criterion. In addition, the loading conditions for the panels are not the same as for the wing box, and so any comparison between the behavior of the compression-loaded panels and the compressed, bent, and twisted wing upper cover panel must take these differences into account.

A method used to predict failure in a damaged, stitched graphite–epoxy structure by examining predicted bending and membrane strains a small distance away from the impact site is described in Ref. 5. This method calculates a so-called ''PDF'' parameter that leads to a predicted failure load. A failure prediction for the damaged single-stringer panel based on this method results in a failure prediction of 95,550 lb. After being subjected to impact damage, the panel was loaded to failure. The panel failed at 94,600 lb of load, or 99% of the failure load predicted by using the method of Ref. 5. For the single-stringer panel, the bending behavior in the region of the impact site significantly influences the failure of the damaged panel.

In single-stringer panels, the interlaminar strain between the stringer flange and the skin and the shear strain in the intercostal flange caused the failure of the undamaged panel. Axial strain near the impact site and the shear strain in the stringer flange caused the failure to occur in the damaged panel.

Multistringer Panels

Three multistringer panels were loaded to failure; however, results for only one multistringer panel, identified as L-2, are presented herein. Results for the other two multistringer panels are presented in Ref. 6 and are summarized in Table 3. Each panel was loaded to a predetermined load, unloaded, and damaged using a dropped-weight impactor, and then loaded to failure. Damage resulted in permanent indentation depths ranging from less than 0.01 to 0.16 in. Impact sites were on the skin near the flange of the tapered stringer away from the spar cap. This location was a point of high strain, but not the point of maximum strain. The point of maximum strain in the skin was in the skin near the tapered stringer and spar cap. A description of the size of the damage inflicted in the panels is given in Table 1. Initial load levels were determined by predicting the load level that would induce the design stress at the planned damage site.

Panel L-2 was initially loaded to 447,000 lb. The panel was not damaged during the initial loading. Axial surface strains predicted by finite element analysis and measured during the initial and final loading are shown in Figs. 12 and 13. Strains located midbay and 4 in. from the top of the panel (away from the tapered stringer and impact site) are shown in Fig. 12. Strains near the impact site are shown in Fig. 13. These strain results are for the loading prior to inflicting damage, for the damaged panel, and for the analysis. Analysis accurately predicts far-field strains and strains at the impact site. Impact damage has a significant effect on the strain within 1 in. of the impact site, but has no effect away from the impact site.

According to the finite element analysis, the maximum axial strain in panel L-2 occurs in the spar cap blade, and does not

exceed the allowable axial strain for loads less than ~650,000 lb. The allowable shear strain is not exceeded for loads less than 900,000 lb. Interlaminar shear and normal strains between the panel skin and stringer flanges do not exceed allowable values for loads less than the failure load and have little effect on failure.

The panel was subjected to impact damage resulting in an indentation with a depth of 0.11 in. The allowable strain of 0.0053 in./in. at the impact site is exceeded for loads greater than 580,000 lb. Applying the method of Ref. 5 results in a predicted failure load of 570,000 lb. The panel failed through the impact site for a load that is ~85% of that predicted by analysis. The panel failed with a stress at the impact site of 44.6 ksi, which is 113% of the design stress. A photograph of panel L-2 after failure is shown in Fig. 14.

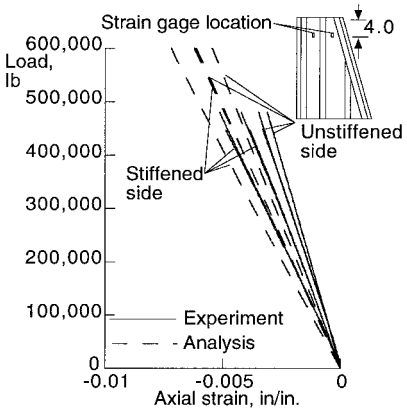

Fig. 12 Axial surface strains in the skin away from the impact site of panel L-2.

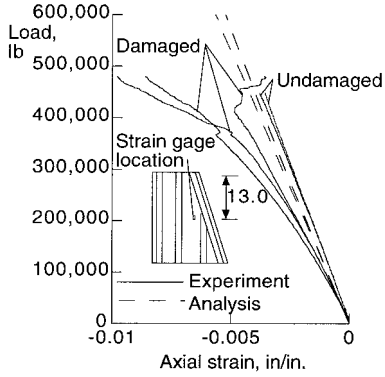

Fig. 13 Axial surface strains in the skin at the impact site of panel L-2.

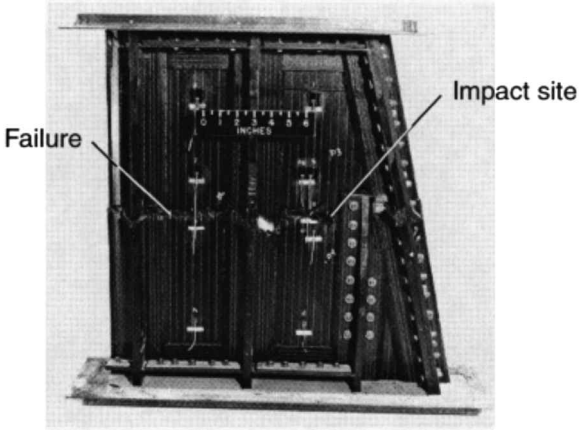

Fig. 14 Failed panel L-2.

Test data indicate that the maximum midplane strain (based on the surface strain gauges) near the impact site reached 0.0053 in./in. for a load equal to 397,000 lb. The panel failed at a load of 484,000 lb. The maximum midplane strain in the region of the impact site was 0.0062 in./in., which is 1.16 times the allowable strain value. The predicted maximum strain in the panel away from the impact site is 0.0058 in./in., which is significantly less than the allowable strain value in an undamaged structure, so that failure was caused by the strain in the region of the impact.

Summarizing the results for panels L-1 and L-3, all multistringer panels failed through the impact site. Interlaminar stresses and bending strains were relatively small in the multistringer panels. The multistringer panels L-2 and L-3 had damage that was less than a 0.11-in.-deep dent failed with more stress in the skin than the design stress value. The most severely damaged panel, L-1, had a dent depth that was 50% deeper than that required to define visible damage, and the panel failed with the stress at the impact site equal to approximately 10% less than the design stress value.

Concluding Remarks

Stitched graphite–epoxy panels were loaded to failure to evaluate the effect of impact damage in panels with a terminated stringer. The terminated stringer is ended by either a reduction in blade thickness or by a reduction in blade height. Panels with a single stringer whose blade contained a gradual reduction in thickness had high values of shear stress in the stringer flange and high values of interlaminar shear stresses between the stringer flange and skin. The maximum interlaminar shear stress in the stringer flange occurs at the end of the flange where it terminates at the intercostal flange. The maximum axial strain, shear strain, and interlaminar strain occur in close proximity, and failure could result from any or a combination of these strains.

Test results for the undamaged single-stringer panel indicate that failure initiates at the interface between the skin and stringer flange. The separation of the stringer flange from the skin occurs immediately beneath the blade of the stringer. The location of failure predicted by analysis is the same as the test panel failure location. The damaged single-stringer panel failed through the impact sites at 99% of the predicted failure load based on predicted membrane and bending strains in the region of the impact site. Significant bending behavior occurs in the single-stringer panels, and they failed with less stress in the skin than the design stress value. The damaged single-stringer panel failed at a stress level that is 10% less than the failure stress of the undamaged single-stringer panel.

Multistringer panels contained a stringer blade that was tapered in height. All multistringer panels were damaged in the skin near the tapered stiffener prior to loading the panels to failure, and all panels failed through the impact site. Interlaminar stresses and bending strains were relatively small in the multistringer panels. Multistringer panels with damage less than a 0.11-in. deep dent failed with more stress in the skin than the design stress value. The most severely damaged panel had a dent depth that was 50% deeper than that required to define visible damage, and the panel failed with the stress at the impact site equal to approximately 10% less than the design stress value.

Stringer terminations with a blade tapered in thickness induce high shear strains and high interlaminar stresses not seen in stringer terminations with the blade tapered in height. Impact damage to the skin of these panels does not appear to cause significantly reduced failure loads.

References

[1]Jegley, D. C., and Bush, H. G., "Structural Test Documentation and Results for the McDonnell Douglas All-Composite Wing Stub Box," NASA TM 110204, April 1997.

[2]Markus, A., Thrash, P., and Grossheim, B., "Manufacturing Development and Requirements for Stitched/RTM Wing Structure," NASA CP 3229, June 1993, pp. 503–523.

[3]Brogan, F. A., Rankin, C. C., and Cabiness, H. D., *STAGS User Manual*, Lockheed Missile and Space Co., P032594, Palo Alto, CA, 1994.

[4]Brewer, J. C., and Lagace, P. A., "Quadratic Stress Criterion for Initiation of Delamination," *Journal of Composite Materials*, Vol. 22, Dec. 1988, pp. 1141–1155.

[5]Hinrichs, S., "General Methods for Determining Stitched Composite Material Stiffnesses and Allowable Strengths, Volume I," McDonnell Douglas Corp., Rept. MDC94K9113, Long Beach, CA, March 1995.

[6]Jegley, D. C., "Behavior of Compression-Loaded Composite Panels with Stringer Terminations and Impact Damage," AIAA Paper 98-1785, April 1998.